Evaporation and cluster abundance spectra

Klavs Hansen[1] and Ulrich Näher[2]
[1]*Institut of Physics and Astronomy, Ny Munkegade, DK-8000 Aarhus C, Denmark*
[2]*Max-Planck-Institut für Festkörperforschung, Heisenbergstrasse 1, 70569 Stuttgart, Germany*
(Received 17 March 1999)

Statistical fragmentation can give valuable information on the internal structure of clusters due to the strong dependence of the evaporation rate on the activation energy for the process. In particular, the abundances in an ensemble of hot clusters will reflect the relative stabilities of the individual species. We derive the relation between evaporative activation energies and relative abundances for large clusters. Quantitative criteria for the applicability of the theory are derived and the analytical results are compared with numerical simulations. [S1050-2947(99)05208-7]

PACS number(s): 36.40.Qv, 36.40.−c, 36.20.Kd

INTRODUCTION

One of the goals of cluster research is to unravel the energetics of clusters. In particular, the homologous series of clusters of the same material have attracted much interest. In these series, the stability often shows characteristic variations with size. These stability variations are almost always manifestations of an underlying shell structure, whether quantal [1–4] or geometrical [5–7] in nature. Both such periodicities and variations in binding energies in general can be effectively probed by evaporative processes. The usefulness of evaporation derives from the strong dependence of the rate constant on the activation energy of the process. Under proper experimental conditions abundances reflect evaporation rates in an unambiguous way. Hence, variations in abundances will reflect variations in activation energy with cluster size. Activation energies, on the other hand, are simply the differential binding energies (separation or dissociation energies) of the clusters provided the transition state is trivial [8]. It is thus in principle possible to transform abundance spectra into curves for separation energies vs size. The problem of relating binding energies to abundances or evaporation probabilities has been addressed previously in a number of papers, either dealing with small clusters or by solving it through numerical calculations of cooling rates [12–14]. Some of the elements of the present analysis were also presented in [15].

The relation between abundances and binding energies has, however, not been known previously, for clusters larger than about 100 atoms. In this work we present the solution of the problem in approximate and simple but still accurate terms. The problem can be stated as follows: Given a collection of free, hot clusters with an abundance distribution which at time zero is smooth and broad, what is the resulting abundance pattern at a later time if separation energies vary with cluster size? The main motivation for this work is to be able to invert abundance spectra to obtain the separation energies. Hence the solution must be simple and easily applicable in the interpretation of the type of experiments described in, for example, [3,6,9–11].

Figure 1 illustrates the key ingredients of the problem. They are (1) a collection of initially hot clusters, and (2) a line representing the final temperatures for each cluster size. The collection of hot clusters moves down to the line of final temperatures at which the abundances are probed at a certain time, defined by the time scale in the experimental setup used to measure the abundances. The sampling time can, for example, be the time for mass separation in a simple time-of-flight mass spectrometer. Each cluster size will capture an amount of the hot ensemble according to the shape of the final-temperature curve. The solution of the problem consists in tracing a unit mass interval at the final temperature back into the initial temperature distribution. The final time abundance reflects the size of the area of the crosshatched initial distribution in Fig. 1 covered by this unit mass interval trace.

This tracing procedure is easily performed for small clusters [16]. For large clusters complications arise. The most important is the determination of the final-temperature curve itself. For both small and large clusters the curve is in principle determined by the separation energies of all the cluster sizes that are encountered during the decays from the initial to the final size. For small clusters, only the last separation energy in this sequence is relevant and this fact facilitates the analysis of evaporative processes enormously. This is not so for large clusters. An indication that the situation is more complicated for large clusters is the fact that the width of the final energy distribution for a large size cluster is larger than the separation energy [17]. This implies that the final temperature is determined by a finite range of evaporations and not just the last one. This in turn means that a given final mass will receive contributions from a broad range of initial

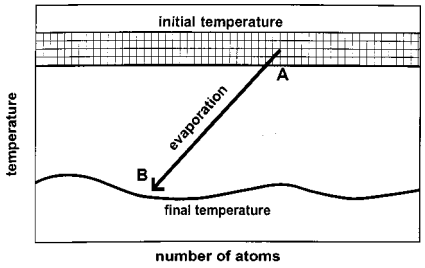

FIG. 1. The principle of the experiments described in the text. The initially hot collection of clusters (*A*) moves down to the more or less well defined final temperature curve (*B*) during the cooling time. The time increases monotonically but highly nonlinearly along the trajectories from *A* to *B*.

masses, even in the case where the initial-temperature distribution is a δ function. The derivation of the proper averaging procedure for this problem constitutes the main calculational content of this work.

In this pictorial formulation of the problem it is also clear that a significant admixture of dimer evaporation will cause severe complications for the solution. When both dimer and monomer evaporation is present, the backpropagation of the final-temperature curve into the initial distribution will in principle depend on all the dimer-monomer branching ratios encountered on the way from initial to final configuration. The fact that these branching ratios are temperature dependent only adds to the complications. The weight of the dimer channel can be judged from tabulated dimer-monomer vapor ratios which also represent the branching ratios of the two evaporative channels for large clusters. The only elements of the first three groups that have any measurable vapor pressure from the dimers are the alkali metals Li, Na, K, Cs, and Rb [18]. The dimer/monomer vapor pressure ratio is in these cases at or below 2×10^{-3} at the relevant temperatures which, as we will see below, is about $\frac{1}{30}$ of the enthalpy of vaporization $[P_{\mathrm{Li}_2}/P_{\mathrm{Li}}(650\,\mathrm{K})=1.9\times10^{-3}$, $P_{\mathrm{Cs}_2}/P_{\mathrm{Cs}}(300\,\mathrm{K})=1.9\times10^{-5}$, for example]. Thus only one in 500 (Li) or 50 000 (Cs) evaporations will be dimer loss. We will therefore exclude dimer evaporation from the analysis. We will, however, include cases where the monomer has internal degrees of freedom, such as the benzene data of [19], but without going into all the details.

We will also leave out a discussion of the effects of radiative cooling on the abundance spectra although thermal radiation influences evaporation rates and thereby also abundance spectra [20]. Radiative cooling is important relative to evaporative cooling mainly for fullerenes and refractory metals at long times where also thermionic emission may be present [21–24]. The precise time scale is material dependent and must be determined by experiment in each case. This work includes tests to check whether radiation or other complications voiding the derived relations are present or not.

The paper is structured as follows. We begin with a brief review of the ''evaporative ensemble'' theory developed by Gspann, Klots, and others [25,26], applicable to small clusters, and derive the abundance spectrum in this limit. Next we address the question of the decay rate in the large cluster approximation and derive a scaled equation for the temporal development of this quantity. The solution of this scaled equation serves as the basis for treating variations in separation energies perturbatively. Then decay rates are related to abundances. This gives the desired result. The validity of the analytical work will be demonstrated by numerical calculations.

RATE CONSTANTS

A treatment of evaporative processes requires that we have established the basics in the form of an expression for the rate constant. Naively we must specify the rate constant with as much precision as we want for the results. If this were really the case, it would cause serious complications for a general and easily applicable solution of the problem. Luckily it is not the case. The reason is that observable rates and abundances will be averages over a wide distribution of energies. Consequently, many of the finer details in the formulation of the rate constants will be averaged out and disappear from the final formulas. The situation is analogous to kinetic gas theory which can be developed without detailed knowledge of the structure of gas molecules. Nevertheless, in order not to antagonize readers unnecessarily, we begin by establishing some useful facts about evaporative rate constants for clusters. Some of the results in this section can be found in [12,27–30].

A convenient formulation of unimolecular reactions for clusters is found in the Weisskopf expression, originally developed for nuclear reactions but well suited for clusters also. It reads (for atomic monomers) [31]

$$k(\epsilon)d\epsilon=\frac{g\mu\sigma(\epsilon)\epsilon}{\pi^2\hbar^3}\frac{\rho_{N-1}(E-D_N-\epsilon)}{\rho_N(E)}d\epsilon \tag{1}$$

for the evaporation of a monomer from cluster N with internal energy E through a process with activation energy D_N. g is the monomer statistical weight, i.e., the spin degeneracy, μ the reduced mass of the channel, in practice very close to the monomer mass, $\rho_N(E)$ the level density of cluster N, and ϵ the kinetic energy in the c.m. system. σ is the atomic capture cross section for the inverse process.

Since ϵ is only a very small part of the total energy, we can use standard procedures and expand the logarithm of ρ_{N-1} to first order in ϵ:

$$\begin{aligned}k&=\int_0^{E-D_N}k(\epsilon)d\epsilon\\&=\frac{g\mu}{\pi^2\hbar^3}\int_0^{E-D_N}\sigma(\epsilon)\epsilon e^{-\epsilon/T_d}d\epsilon\frac{\rho_{N-1}(E-D_N)}{\rho_N(E)},\end{aligned} \tag{2}$$

where the (daughter) temperature T_d is defined as usual:

$$T_d^{-1}=\frac{d\ln[\rho_{N-1}(E-D_N)]}{dE} \tag{3}$$

($k_B=1$). The cross section σ may be energy dependent as indicated. If not simply a geometric cross section

$$\sigma=\sigma_N=\pi(r_N+r_1)^2=\pi r_1^2[(N-1)^{1/3}+1]^2\approx\pi r_1^2N^{2/3} \tag{4}$$

one expects a cross section of the type

$$\sigma=\sigma_N\left(1-\frac{V(r_N)}{\epsilon}\right), \tag{5}$$

where $V(r_N)$ is the potential at the capture radius of the cluster. Alternatively the cross section may arise from a purely point particle attractive potential,

$$\sigma\propto\epsilon^{\alpha}, \tag{6}$$

where $\alpha\geqslant-\frac{1}{2}$, or possibly a hybrid type of two of these. In any case the cross section is multiplied with ϵ and integrated with the Boltzmann factor. This leaves us with a temperature dependence that amounts to a power law with a small power or possibly a sum of two such terms. A reverse activation

barrier would be reflected in a threshold value for the cross section with respect to ϵ or equivalently as a renormalization of the dissociation energy which would be the sum of the adiabatic separation energies and the reverse activation barrier. We expect that dissociation energies and separation energies are identical, at least for most metal and the noble gas clusters. The question can in principle be settled by measuring the ϵ distribution. To be specific we will in the following take the geometric cross section $\sigma_N = \pi r_s^2 N^{2/3}$ for our large clusters.

The rate constant with the geometric cross section is

$$k_N(E,D_N) = \frac{g\mu\sigma_N}{\pi^2\hbar^3} T_d^2 \frac{\rho_{N-1}(E-D_N)}{\rho_N(E)}. \tag{7}$$

The ratio of level densities, $\rho_{N-1}(E-D_N)/\rho_N(E)$, can be expressed in terms of the level density of cluster size N by the approximate relation, using the Debye temperature $T_D = \hbar\omega_D$,

$$\rho_{N-1}(E-D_N)\left(\frac{T_d}{T_D}\right)^3 \approx \rho_N(E-D_N). \tag{8}$$

To the extent that $T_D/\hbar$ represents an average of the vibrational frequencies in the cluster, the approximation is asymptotically exact in the harmonic oscillator approximation in the high temperature limit for large N. Since this is the limit we are interested in, we will adopt the approximation. Hence

$$k_N(E,D_N) = \frac{g\mu\sigma_N}{\pi^2\hbar^3} \frac{T_D^3}{T_d} \frac{\rho_N(E-D_N)}{\rho_N(E)}. \tag{9}$$

The quantity $\omega' \equiv g\mu r_1^2 T_D^2/\pi\hbar^3$ has dimension of frequency. We can then write the rate constant in the simpler form

$$k_N(E,D_N) = \omega' N^{2/3} \frac{T_D}{T_d} \frac{\rho_N(E-D_N)}{\rho_N(E)}. \tag{10}$$

For sodium, for example, where $g=2$, $\mu = 23$ amu, $T_D = 0.013$ eV, and $r_1 = 4.0a_0$, the value of ω' is $4\times10^{15}\,\mathrm{s}^{-1}$. For monomer evaporation from diamond with $T_D = 0.16$ eV and $r_1 = 1.6a_0$, $\omega' = 1\times10^{17}\,\mathrm{s}^{-1}$ (geometrical cross section value).

As we will see below, the value of T_d does not change much during experimental time scales and the change in T_D/T_d can be neglected without significant loss of precision. Hence we have the prototype expression for a rate constant (with $\omega = \omega' T_D/T_d$):

$$k_N(E,D_N) = \omega N^{2/3} \frac{\rho_N(E-D_N)}{\rho_N(E)}. \tag{11}$$

Rate constants in this form can be approximated even more. We will later need the derivative of the rate constant with respect to energy. For this purpose we calculate the logarithmic derivative of the ratio of level densities:

$$\frac{d\ln[\rho_N(E-D_N)/\rho_N(E)]}{dE} = \frac{1}{T_d} - \frac{1}{T_m}, \tag{12}$$

with a self-explanatory definition of T_m. Using the average of the two temperatures, $T = (T_m + T_d)/2$, the logarithmic derivative can be approximated as

$$\begin{aligned}\frac{d\ln[\rho_N(E-D_N)/\rho_N(E)]}{dE} &= \frac{1}{T - D_N/2C_v} - \frac{1}{T + D_N/2C_v} \\ &= \frac{D_N}{C_v T^2} + O\left(\frac{1}{T}\left(\frac{D_N}{2C_v T}\right)^3\right),\end{aligned} \tag{13}$$

where we have used

$$T_d = T(E-D_N) \approx T(E - D_N/2) - \frac{D_N}{2}\frac{1}{C_v}, \tag{14}$$

and analogously for T_m. An important point concerning the temperature T is that for constant heat capacity, $dT/dE = 1/C_v$. The heat capacity needs only be constant over a temperature interval of $D_N/2C_v$, a requirement easily met for large clusters.

It is also easy to express the rate constant in terms of T. By expanding the logarithm of the level density around $E - D_N/2$ one gets

$$\begin{aligned}\rho(E-D_N) &= \rho(E - D_N/2)\exp\left(-\frac{D_N}{2}\frac{d\ln(\rho)}{dE} + \frac{D_N^2}{8}\frac{d^2\ln(\rho)}{dE^2} + \cdots\right) \\ &\approx \rho(E - D_N/2)\exp\left(-\frac{D_N}{2T} - \frac{D_N^2}{8T^2 C_v}\right)\end{aligned} \tag{15}$$

and

$$\begin{aligned}\rho(E) &= \rho(E - D_N/2)\exp\left(\frac{D_N}{2}\frac{d\ln(\rho)}{dE} + \frac{D_N^2}{8}\frac{d^2\ln(\rho)}{dE^2} + \cdots\right) \\ &\approx \rho(E - D_N/2)\exp\left(\frac{D_N}{2T} - \frac{D_N^2}{8T^2 C_v}\right).\end{aligned} \tag{16}$$

The ratio of the two reduces to

$$\frac{\rho(E-D_N)}{\rho(E)} \approx \exp(-D_N/T). \tag{17}$$

This approximation is essentially the so-called ''finite heat bath method'' of Klots. It is particularly well suited for large cluster since the relative error is a factor on the order of $1 - \exp(-D_N^3/T^3 12C_v^2) \approx -D_N^3/(T^3 12C_v^2)$ which is very small as we will see.

The final result for the rate constant is the simple expression

$$k_N = \omega N^{2/3} \exp\left(-\frac{D_N}{T}\right). \tag{18}$$

We note that the expression implies that the rate constants can be parametrized by a single quantity with dimension energy, D_N. As discussed in [29,32], this energy need not refer to the transition between mother and daughter clusters in their ground states. Rather it must represent a properly defined free energy.

THE SMALL CLUSTER LIMIT

The special features of a theory based on statistical decay arise from the fact that under usual experimental conditions the observation time is many orders of magnitude larger than $1/\omega$. In practice the experimental time scale often has a lower limit given by the time it takes to accelerate ions and separate them in an electric field. This time is typically several hundred ns. This indicates a very low value of T/D. As a consequence of this and the strong temperature dependence of the rate constant there is a rather well defined upper limit for the temperature of small clusters. This limit can be found simply by equating the rate constant k to the inverse cooling time t. This yields

$$T_{\max,N}=\frac{D_N}{\ln(N^{2/3}t\omega)}. \tag{19}$$

For clusters initially at a sufficiently high temperature, there is also a well defined lower limit for the temperature. If the clusters have undergone at least one evaporation, the only way a cold cluster of size N can be produced is by evaporation from a warmer cluster of size $N+1$. For the case of small clusters, the effective lowest temperature of a certain size is given by the effective highest temperature of the preceeding size by energy conservation:

$$T_{\min,N}=T_{\max,N+1}-\frac{D_{N+1}}{C_\nu}. \tag{20}$$

The lower limit on the cluster temperature reflects that it is not possible to produce clusters any colder through evaporation because the rate for these processes would be much too small to be observed. This result of course relies crucially on the assumption that all clusters have evaporated at least one atom. The expression Eq. (20) abuses the simple Arrhenius-like rate constant derived above for big clusters. More realistic formulas give surprisingly similar results and we will therefore just continue as if Eq. (18) applies for small clusters also. If the initial distribution is sufficiently smooth, the interval between these two extremes will be populated with equal density. Then the temperature distribution is practically a square box and abundances I_N can be approximated by

$$I_N\propto T_{\max,N}-T_{\min,N}\simeq\frac{D_{N+1}}{C_\nu}-\frac{1}{\ln(N^{2/3}t\omega)}\Delta_1 D_N \tag{21}$$

or

$$I_N\propto D_{N+1}-\frac{C_\nu}{\ln(N^{2/3}t\omega)}\Delta_1 D_N, \tag{22}$$

where we have defined the first difference as

$$\Delta_1 D_N\equiv D_{N+1}-D_N. \tag{23}$$

(For details on the distribution beyond the square box approximation, see, e.g., [33].) The derived formula of course assumes that $T_{\min,N}$ is non-negative as calculated. That will normally be the case, except for the very smallest clusters. Furthermore, we have ignored the kinetic energy carried away by the fragment. The most important effect of including it will be a change in the absolute energy scale by a few percent. We will ignore it also in the following.

Some remarks on this small N result are appropriate since they also apply to the results derived for large clusters. First it should be noted that it is only possible to find local variations in separation energy by this method. The relation is only a proportionality which is obvious for dimensional reasons. The constant of proportionality is related to the density of the initial, high temperature size distribution (i.e., region A in Fig. 1). Hence the constant of proportionality will change smoothly across the envelope of the distribution from zero through a maximum and back to zero again at the size where the envelope of the distribution vanishes again. As a consequence it is only possible to apply the formula to abundance variations that occur over a size range which is small compared to the total width of the size distribution.

Furthermore, we see that the abundances are not determined by the total cluster free energy, as would be the case for a situation with clusters in equilibrium with a heat bath. Neither will the differential binding energy (which is essentially the separation energy) determine the abundance spectrum. This would have been the situation if the clusters were in contact with a heat bath but otherwise free as in [34]. Rather, the energy content (temperature) of a specific cluster size is determined by the temperature of the precursor(s) in the decay chain. This is the reason the first difference of the separation energy is relevant in determining the abundance spectrum. This fact is a property of the ensemble, i.e., free clusters without any energy exchange with the environment except the one connected with the evaporative cooling.

In Eq. (22) the prefactor of the difference term is quite large. We will not go into a discussion of the relative magnitude of the two terms in the equation when applied to specific systems. Suffice it to point out that for clusters displaying shell structure the second term often dominates the variations in the first term by a large factor. It can also be seen from Eq. (22) that the structure in the abundance spectra is only weakly time dependent. Taken at face value, the largest structure is actually observed for short times, an observation which was also made in [13]. This result is rather surprising since one would intuitively expect stability patterns to be manifested more strongly the lower the temperature. In reality the picture is not so clear. Short times and hence high temperatures will tend to smear out the structure in the separation energies themselves (for the case of fermionic shell structure, see, e.g., [35–37]) and the resulting amplitude in the abundance spectrum will be a combination of the two effects.

Finally we note that from Eq. (19) and Eq. (21) it is simple to derive a mean decay constant. With a natural definition, the value for size-independent separation energies is

$$k_N \equiv -\frac{dT_{\max}/dt}{T_{\max}-T_{\min}} = \frac{C_v}{[\ln(N^{2/3}\omega t)]^2} t^{-1}. \tag{24}$$

This expression is similar to the one we will derive for large clusters.

ENSEMBLE RATE CONSTANTS FOR LARGE CLUSTERS

The simple derivation of the preceding section depended crucially on the existence of a highest energy, or temperature, in the ensemble, Eq. (19). But as we have shown previously, the assumption of a sharp upper limit on the energy distribution is not valid for clusters that contain more than a few hundred vibrational degrees of freedom [17]. The reason is that for big enough clusters, the change in temperature caused by one evaporation is so small that two consecutive rate constants do not differ much. Clusters at an initial energy E may end up being observed as cluster size $N+1$, N, $N-1$, $N-2$, or as some other size at the sampling time. This width in the number of evaporated atoms is equivalent to a width in the final cluster energy since each evaporation removes one dissociation energy. And since the width of the energy distribution of the small clusters is on the order of one dissociation energy [see Eq. (20)], the smearing in energy becomes important for all cluster sizes for which several evaporations have to be considered. Quantitatively, the limit of validity of Klots's theory was found to be the size

$$N_\kappa = \frac{1}{3}\left(\frac{D}{T}\right)^2 \simeq 200-300, \tag{25}$$

where, to be specific, we used $C_v = 3N-6 \approx 3N$. Above this limit it is a poor approximation to assume that two consecutive rate constants are vastly different. Rather a theory must be based on the opposite approach; that they are almost equal.

Since the width of the temperature distribution is quite narrow for large clusters, we can approximate the distribution by its mean value. Both the rate constant and the temperature for a specific size N can at a given time be represented by a single value, k_N and T_N. In general this decay constant is size dependent since the separation energies are size dependent. An important partial goal is to find this size dependence in terms of variations of the separation energies. In order to do this we will first find the decay rates for the case of size-independent separation energies. That solution will then serve as the starting point for a perturbative expansion in the variations.

Consider the temporal development of the decay constant for a given cluster as it evaporates atoms. Since the clusters are large we can approximate finite differences by derivatives and vice versa. Then the Boltzmann factor $B_N \equiv \exp(-D_N/T_N)$ develops according to

$$\frac{dB_N}{dt} = B_N \frac{D_N}{T_N^2}\frac{D_N}{C_v}(-k_N) - \frac{\Delta_1 D_N}{T_N} B_N(-k_N), \tag{26}$$

where we have used $dT_N/dN = D_N/C_v$, $dN/dt = -k_N$, and Δ_1 is defined as in Eq. (23). This differential equation holds also when the monomeric unit has internal degrees of freedom and carries thermal excitation energy away in addition to the separation energy. The correction is of order $\Delta_1 C_v/C_v$ relative to the leading terms on the right-hand side of Eq. (26). For sufficiently small variations in separation energy with size, the dominating change in B_N is given by the first term on the right-hand side of Eq. (26). If we ignore the last term and denote B_N, k_N, and T_N pertaining to the special solution for $D_N = D$ by B, k, and T, respectively, the equation becomes

$$\frac{dB}{dt} = -\frac{1}{C_v}\left(\frac{D}{T}\right)^2 Bk \tag{27}$$

or

$$\frac{dB}{d\tau} = -B^2(\ln B)^2, \tag{28}$$

where the reduced time is defined as

$$\tau \equiv \frac{\omega t N^{2/3}}{C_v}. \tag{29}$$

The equation can be solved to give the asymptotic series

$$\frac{1}{B(\ln B)^2}\left(1 - \frac{2}{\ln B} + \frac{6}{(\ln B)^2} + \cdots\right) = \tau + \tau_0. \tag{30}$$

In the relevant limit where $-\ln B \gg 1$, this can be approximated by

$$\frac{1}{B}\frac{1}{(\ln B)^2} = \tau + \tau_0, \tag{31}$$

where τ_0 is the left-hand side of Eq. (30) evaluated at $t=0$ [38]. The condition that the clusters are initially very hot can be stated quantitatively as $B(0) \gg B(\tau)$. The translation of this inequality into a condition on temperature was discussed in [17] and found to impose a surprisingly mild requirement on the initial temperature. Assuming this requirement is indeed fulfilled, τ_0 will be close to zero and the expression reduces to

$$(\ln B)^2 B = \tau^{-1}. \tag{32}$$

From this follows immediately the prediction that

$$k = \frac{C_v}{(\ln B)^2} t^{-1}, \tag{33}$$

which was also derived in [17] with different means. As a first approximation, $(\ln B)^2$ can often be set equal to $[\ln(\omega t N^{2/3}/C_v)]^2$. This defines

$$N_\kappa = \frac{N(\ln B)^2}{C_v} \tag{34}$$

in a slightly more general sense than in [17].

The next step is to add size dependence to the separation energies. The effect on rate constants can be calculated by retaining the difference term of the D_N's in Eq. (26). Rewriting the equation in terms of the scaled time τ it reads

$$\frac{dB_N}{d\tau} = -B_N^2(\ln B_N)^2 - B_N^2 \ln B_N C_v \frac{\Delta_1 D_N}{D_N}. \tag{35}$$

Varying separation energies are most efficiently handled by introducing the function H_N:

$$B_N = B/H_N. \tag{36}$$

Substituting this into Eq. (35) and assuming that $|\ln B| \gg |\ln H_N|$ as well as $|\ln B| \gg 1$, yields an equation for the temporal development of H_N:

$$\frac{dH_N}{d\ln\tau} = -(H_N - 1) + \frac{\Delta_1 D_N}{D_N} \frac{C_v}{\ln B(\tau)}. \tag{37}$$

This is easily solved to give

$$H_N - 1 = -\int^{\ln\tau} d\ln\tau' \frac{\tau}{\tau'} \frac{\Delta_1 D_{N'}}{D_{N'}} \frac{C_v'}{\ln B'}. \tag{38}$$

Since $d\ln\tau = dN/C_v(\ln B)^2$, Eq. (38) can be transformed into

$$H_N - 1 = -\int^N dN' \frac{\tau'}{\tau} \frac{\Delta_1 D_{N'}}{D_{N'}} \ln B'. \tag{39}$$

With the linear expansion

$$\ln\tau' = \ln\tau + \frac{N' - N}{C_v}(\ln B)^2 \tag{40}$$

and neglecting the N dependence of $\ln B'$ this yields

$$H_N - 1 = \ln B \int^N dN' \frac{\Delta_1 D_{N'}}{D_{N'}} \exp\left(\frac{N - N'}{C_v}(\ln B)^2\right) \tag{41}$$

or, in the discrete version,

$$H_N = 1 + \ln B \sum_{N'=N}^{N_0} \frac{\Delta_1 D_{N'}}{D_{N'}} \exp\left(\frac{N - N'}{C_v}(\ln B)^2\right). \tag{42}$$

(N_0 is the initial size of the cluster.) The expression for k_N then becomes

$$k_N = \frac{k}{1 + \ln B \sum_{N'=N}^{N_0} (\Delta_1 D_{N'}/D_{N'}) \exp\{[(N - N')/C_v](\ln B)^2\}}. \tag{43}$$

The result can be understood as follows: The change from the unperturbed value of k into k_N is induced by a source term of the form $-\Delta_1 D_N/T_N \simeq \ln B \Delta_1 D_N/D_N$; a change in the separation energy will change the separation energy-temperature ratio away from the solution given by k. A positive value of $\Delta_1 D_N$, e.g., will lower the value of H_N and increase the decay constant ($\ln B$ is negative). With this higher rate, the cluster will cool faster. This faster cooling acts as a negative feedback and provides an efficient focusing mechanism for the rate constant to bring it back to the universal attractive curve, given by the function k. It takes, however, a finite number of evaporative cooling steps to return to the universal curve. This number is given by $C_v/(\ln B)^2 = N/N_\kappa \approx N/300$. All changes of the separation energy within that size interval will influence the value of k_N. Thus, to obtain a fully developed evaporative spectrum, the number of evaporated atoms must be larger than N/N_κ. As discussed below this limit is not just a necessary condition, it is also sufficient. The requirement is the same as the one previously mentioned for the unperturbed solution for B, i.e., an initial temperature which is about 10–20% above the final. In the following we will assume that this ''evaporative equilibrium'' is reached and just stress that the assumption has to be verified in an experimental situation.

The expression for H_N can quite often be approximated further. When the variations in D_N are sufficiently smooth, which is often the case for large clusters, the derivative factor can be set to a constant in the summation. Then the summation simply gives the factor $N/N_\kappa = C_v/(\ln B)^2$ and the function reduces to

$$H_N = 1 + \frac{\Delta_1 D_N}{D_N} \frac{C_v}{\ln B} \tag{44}$$

and thus

$$k_N = \frac{k}{1 + (\Delta_1 D_N/D_N)(C_v/\ln B)}. \tag{45}$$

All these results are based on a perturbative expansion of the equation that determines the temporal development of the rate constant. This treatment breaks down when the perturbations are large, i.e., when dissociation energies change abruptly. When this happens, two different approximations used in the present derivation can fail. One is the linearization

$$\left[\exp\left(\frac{\Delta_1 D_N}{T_N}\right) - 1\right] \to \frac{\Delta_1 D_N}{T_N} \tag{46}$$

when the finite difference is substituted by the continuous derivative to arrive at Eq. (26). The validity of the simple expressions is then limited to cases where $|\Delta_1 D_N/T_N| \ll 1$, i.e., where the change in separation energy is less than a few percent for each mass unit. Should a situation arise when this limit is exceeded, the solution can be improved simply by avoiding the above linearization. The results of this section prevail with the obvious substitutions. In any case one is safe if relative changes in neighboring abundances are less than a factor of N/N_κ which can be seen from the results found below.

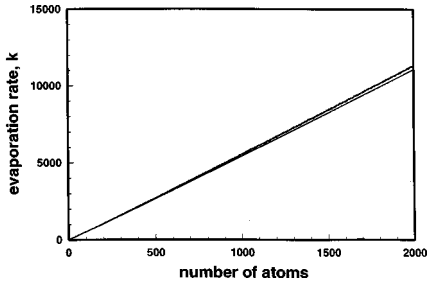

FIG. 2. The rate constant (in s^{-1}) for constant separation energies and $\omega=10^{15}\,s^{-1}$, $t=10^{-5}$ s. Notice the almost linear behavior. The slightly fluctuating curve is the outcome of a MC simulation. The analytical curve is calculated using Eq. (30) with $\tau_0=0$. It also includes a correction due to the decrease in the number of degrees of freedom at each evaporation. It is treated perturbatively, yielding $H_N=1+3/\ln B$. In applications, Eq. (32) will normally be sufficient since only the logarithm of the Boltzmann factor is needed. This last approximation was adhered to in Figs. 4–6. The curves contain no fitted parameters.

The other limit of the theory arises when the value of $\Delta_1 D_N/D_N$ is positive and large. We see from Eq. (44) that the approximate treatment requires that H_N should not approach zero. In other words, the approximation is valid for $\Delta_1 D_N/D_N \lesssim -\ln B/C_v$. The physical situation which renders this inequality invalid is a decrease in separation energy with each evaporation which is large enough to compensate for the decrease in temperature. In the picture where abundances are determined by a projection of the initial distribution onto the final temperature, this corresponds to a complete shadowing of certain cluster sizes by some precursor in the decay chain. This limitation is also present in the small cluster limit. It is equivalent to the requirement that $T_{\min,N}$ is positive as calculated. Although the limitations outlined here may be exceeded (for examples see [39,40]), these cases are still so rare that they are best treated on an individual basis.

In order to illustrate the analytical results, we have simulated a series of decay chains by Monte Carlo calculations. In Fig. 2 we compare the analytical and the simulated value of k for constant separation energies. Figure 3 shows two examples of calculated and simulated rate constants for size-dependent separation energies.

RATE CONSTANTS AND ABUNDANCES

In order to relate the rate constants derived above to abundances, we will first establish the corresponding relation for a single decay chain. This greatly simplifies the problem since in a specific decay chain the initial temperature and hence all decay rates are fixed, provided we ignore the stochastic nature of the small kinetic energy carried by the fragment. The only stochastic element in a decay chain is then the time at which the evaporations in the chain occur. Consider the simultaneous distribution of decay times in a chain starting at size N_0:

$$P(t_N,t_{N+1},\ldots,t_{N_0})\prod_{j=N}^{N_0} dt_j=\prod_{j=N}^{N_0} k_j e^{-k_j t_j} dt_j\,. \qquad (47)$$

Here t_j is the time since cluster j was produced by evaporation from size $j+1$. The probability that size N decays into

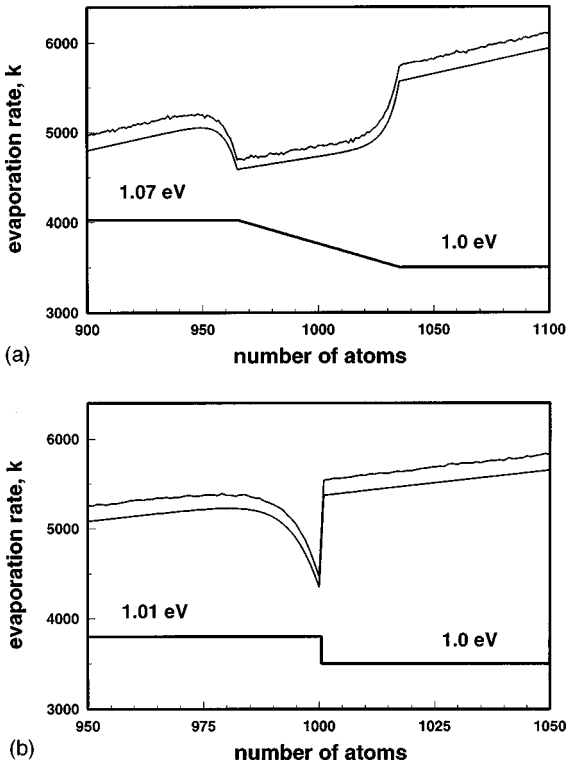

FIG. 3. Average rate constants for size-dependent separation energies (in s^{-1}). The slightly fluctuating curve is the result of MC simulations. The other is the prediction of Eq. (43). Also included are the separation energies used in the calculations. Both figures show clearly the importance of the difference term in Eq. (43). The transient effect of a nonzero difference term is also clearly visible. The curves contain no fitted parameters.

size $N-1$ at time t is the integral of this distribution with respect to all the intermediate lifetimes with the restriction that these are positive and sum up to t:

$$k_N I_N=\int_0^\infty \delta\left(\sum_{j=N}^{N_0} t_j - t\right)\prod_{j=N}^{N_0} k_j e^{-k_j t_j} dt_j\,. \qquad (48)$$

Expressing the δ function as the Fourier transform of 1,

$$\delta(t)=\frac{1}{2\pi}\int_{-\infty}^{\infty} e^{-ikt}dk, \qquad (49)$$

the integrations of the individual decays decouple and are easily performed to give

$$k_N I_N=\frac{1}{2\pi}\int_{-\infty}^{\infty} dk\, e^{ikt}\prod_{j=N}^{N_0}\frac{k_j}{k_j+ik}. \qquad (50)$$

The product under the integral sign is the Fourier transform of the desired probability. It has the nice property that it factors into functions that depend only on the individual decay constants. The integral can be calculated by the method of residues and the result is useful for numerical simulations as an alternative to Monte Carlo simulations:

$$k_N I_N=\sum_{j=N}^{N_0} k_j e^{-k_j t}\prod_{n\neq j}\frac{k_n}{k_n-k_j}. \qquad (51)$$

A few examples of numerical simulations using this formula can be found in [15]. By a saddle point expansion of the integrand of Eq. (50) and an evaluation of the higher order terms, it is possible to obtain the result in [17] of a normal distribution in time for the product $k_N I_N$ also for the case of $\Delta_1 D_N \neq 0$.

To understand the behavior of Eq. (50) consider the effective range of k values in the integrand. Since the clusters are large, there will be N/N_κ similar rate constants appearing in the product under the integral sign. Hence for values of k larger than typically $(N_\kappa/N)^{1/2}k_N$ the integrand will be suppressed. Consequently the ratio k/k_N can be considered a small quantity when integrating. This can be used to evaluate the derivative of I_N with respect to k_N:

$$\frac{\partial I_N}{\partial k_N} = \frac{1}{2\pi k_N}\int_{-\infty}^{\infty} dk\, e^{ikt}\left(\prod_{j=N}^{N_0}\frac{k_j}{k_j+ik}\right)\frac{1}{k_N+ik}. \quad (52)$$

Expanding the last term in the integrand,

$$\frac{1}{k_N+ik} = \frac{1}{k_N} - \frac{ik}{k_N^2} - \frac{k^2}{k_N^3}\cdots, \quad (53)$$

yields the equation

$$\frac{\partial I_N}{\partial k_N} = \frac{I_N}{k_N} - \frac{1}{k_N^2}\frac{\partial I_N}{\partial t} + O\left(\left(\frac{N_\kappa}{N}\right)^{3/2}\right). \quad (54)$$

The second term is of order N_κ/N for a single decay chain. But when decay chains are summed to an ensemble the value reduces significantly due to a cancellation of the derivative term. By the order-of-magnitude estimate

$$\frac{\partial I_N}{\partial t} \approx k_N \frac{\partial I_N}{\partial N} \quad (55)$$

and the observation that k_N only varies by

$$\sigma_{k_N} \approx \sigma_E \frac{dk_N}{dE} \approx \left(\frac{N_k}{N}\right)^{1/2} k_N, \quad (56)$$

one sees that the ensemble average of the time derivative term is zero to leading order in $\sqrt{N_\kappa/N}$;

$$\sum_N \frac{1}{k_N^2}\frac{\partial I_N}{\partial t} \approx \sum_N \frac{1}{k_N}\frac{\partial I_N}{\partial N} = 0. \quad (57)$$

The resulting approximation of Eq. (55),

$$\frac{\partial I_N}{\partial k_N} \approx \frac{I_N}{k_N}, \quad (58)$$

is solved to give

$$k_N I_N = \text{const}. \quad (59)$$

We emphasize that this result is only applicable for large N. It can be interpreted as a steady-state condition for a decay chain but it should be kept in mind that the effective temperature of the k_N's varies with N.

At this point, the only missing ingredient is to sum decay chains over all possible initial conditions. We will perform this summation in analogy to the procedure used in [17] and similar to the summation in Eq. (57), that is, by covering the (N,T) plane densely with decay chains. This summation is trivial apart from a single, minor complication. The complication is related to the density of decay chains that terminate at size N. This density is proportional to the separation energy since the slope of the curves in the (N,T) plane is proportional to the separation energy. Similarly, the volume of the initial distribution projected into the final temperature is inversely proportional to the separation energy of the initial cluster size. Hence

$$I_N \propto \frac{D_N}{D_{N_0}}. \quad (60)$$

The appearance of D_{N_0} in this expression is an unwelcome feature. It will rarely be known from which sizes the decay chains originate. We believe, however, that this problem will not be present under realistic experimental conditions, primarily because the amount of evaporated atoms will be a fairly broad distribution. If this is indeed the case, initial sizes will be averaged over a broad mass interval and hence one can substitute the value of D_{N_0} with the mean value D. Hence

$$I_N \propto D_N. \quad (61)$$

In order to test these results numerically, we show in Fig. 4 examples of abundance spectra, calculated using Eq. (64) derived below, i.e., $I_N \propto D_N k_N^{-1}$ where k_N is determined by Eq. (43).

As we have seen earlier, in order for k_N to reach the evaporative equilibrium value the number of evaporations has to be on the order of N/N_κ or bigger. It might be argued that the number of atoms evaporated needs to exceed any scale over which one wants to determine the structure. For example, probing clusters with shell structure, one might suspect that it would be necessary to evaporate at least one shell in order to see the fully developed evaporative pattern. This intuition is wrong. Figure 1 provides the answer without much further consideration. If the initial and final temperatures are separated by more evaporations than a few times N/N_κ, the projection onto the final temperature will be independent of the initial temperature. This is demonstrated by the simulations shown in Fig. 5 where we have introduced a separation energy of the slowly varying type. The abundance spectra were simulated with different initial temperatures around the theoretical critical value. The results demonstrate that the simple reasoning using Fig. 1 is sufficient and that N/N_κ evaporations indeed suffice to reach evaporative equilibrium.

DISCUSSION

All the ingredients are now available to express the abundances as functions of the separation energies. With the results from the preceding section, Eqs. (59) and (60):

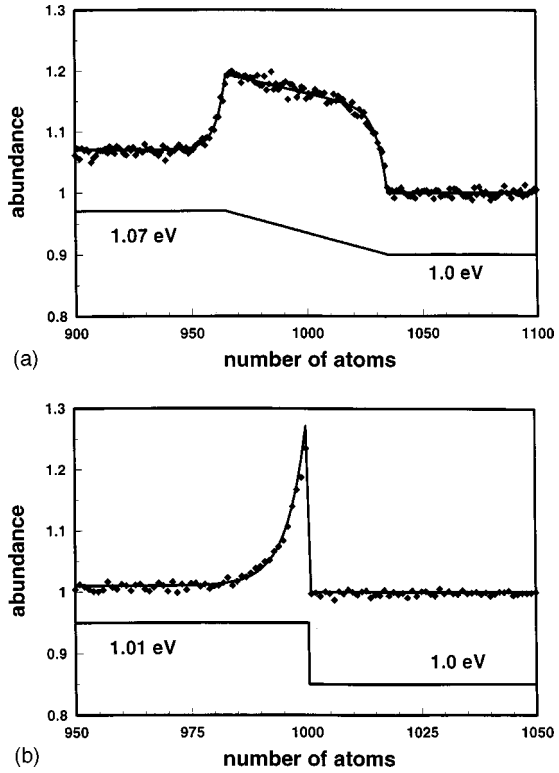

FIG. 4. The relative abundances for the data shown in Fig. 3. The diamonds are the MC-simulated results and the line the analytical result of Eq. (64). Only the overall scales have been matched.

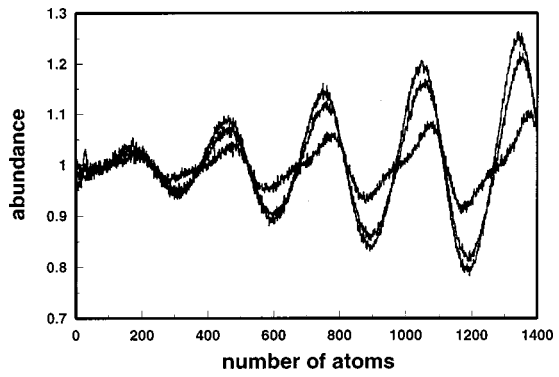

FIG. 5. The development of evaporative equilibrium with initial temperature. The separation energy is $D_N = 1 + 0.05 \sin(2\pi N/300)$. The three spectra result from simulations with initial temperatures equidistantly spaced: $T_0 = 0.038$, 0.044, and 0.050 times the mean separation energy. The amplitude in the spectra increases with initial temperature. The analytical mean final temperature is $0.0372 D_N$ around $N = 100$ and $0.0387 D_N$ around $N = 2000$. With the criterion that the initial and final temperatures should be separated by 10%, the critical initial temperature is then around 0.044. We see indeed that the spectrum is almost completely developed at that temperature. The number of evaporated atoms is much less than the period of 300 in the separation energy; at $N = 1000$, the number is $\Delta N = 35$ for the initial temperature of 0.050. The linear increase in amplitude with size is also clearly visible. The increase is linear even though the amplitude factor on the sine factor is constant. The small feature in the spectra at small sizes is an artifact of the sharp initial temperature. It disappears with a finite width.

$$I_N \propto \frac{D_N}{D_{N_0}} \frac{1}{k_N} = \frac{D_N}{D_{N_0}} \frac{H_N}{k}. \tag{62}$$

Introducing the expression for H_N, leaving out the smooth function k and assuming that D_{N_0} can be substituted by a smooth function of N as discussed [Eq. (61)] yields

$$I_N \propto D_N \left[1 + \ln B \sum_{N'=N}^{\infty} \frac{\Delta_1 D_{N'}}{D_{N'}} \exp\left(\frac{N - N'}{C_v} (\ln B)^2 \right) \right]. \tag{63}$$

For $\Delta_1 D_N / D_N \ll 1$ this expression can to a good approximation be rewritten as

$$I_N \propto D_N + \ln B \sum_{N'=N}^{\infty} \Delta_1 D_{N'} \exp\left(\frac{N - N'}{C_v} (\ln B)^2 \right). \tag{64}$$

It is quite instructive to compare this result to the analogous result for small clusters, Eq. (22). Since the physical situation and thus the mathematical derivation of the abundances are different for the two cases of large and small cluster, it is surprising that the two results are so similar. In both expressions Eqs. (22) and (64) the separation energy appears as one term and the derivative of separation energy with respect to size for the precursors as the second. For the large clusters a sum over a range of precursors is required, whereas for the small ones the last precursor alone is enough to determine the abundance. The constant of proportionality is different in the two cases and this difference reflects the completely different approaches to the problem that are necessary in the two limits. But under certain circumstances even this difference vanishes almost completely. These situations are the same ones that render Eq. (45) valid. If this is used also in the formula for the abundances, the above approximates to

$$I_N \propto D_{N+1} + \frac{C_v}{\ln B} \Delta_1 D_N. \tag{65}$$

The only difference between this expression and the one for small clusters, Eq. (22), is the denominator in the second term, and for values of N close to N_κ, i.e., where the two limits change guard, the two denominators $\ln(\omega t N^{2/3})$ and $-\ln B$, are in fact identical. For smaller N the difference between these two denominators is approximately $\ln(N/N_\kappa)$ which considering the magnitude of the term itself is an acceptable correction. This smooth interpolation between large and small is also seen in the rate constants in Fig. 2. The large N expression is seen to fit the average rate to the very smallest sizes.

We are then in the situation that the desired expression is the same in the small and in the large size limit. We have not derived any results for the intermediate size range. Although mathematically speaking one can imagine infinitely many interpolations between the two limits, physical reason suggests the simple choice that the relation which holds for both large and small clusters should also hold for intermediate sizes. This reasonable hypothesis has held in numerical simulations so far.

The results in Eqs. (63)–(65) differ from the relation which was introduced in [41] between binding energies and abundances and which was used in several papers on electronic shell structure. Abundances were assumed proportional to the rate constants which were evaluated at a size-independent temperature. This unfounded hypothesis was unfortunately assisted by a remarkable coincidence of abundances and theoretically calculated dissociation energies. As shown here the agreement is fortuitous.

The type of experiments for which the present theory is developed, i.e., a sudden excitation followed by a delayed sampling, is by no means the only one where evaporative equilibrium can be used as a diagnostic technique. Alternative to instantaneous heating and subsequent cooling, one can heat the cluster beam continuously and monitor the steady-state abundances. Without going into details, we will just state that the abundance-separation energy relation in this situation is quite similar to the instantaneous heating case. This is most easily seen by following the destiny of a single cluster as it absorbs photons and evaporates atoms. In addition to separation energies, the abundances will then depend on the (possible size-dependent) photon absorption cross section σ_N;

$$I_N \propto \frac{1}{\sigma_N}\left(D_{N+1}+\frac{C_v}{\ln B}\Delta_1 D_N\right). \tag{66}$$

The cooling time that determines B via Eq. (32) is here simply the average time between evaporations.

CONCLUSION

We will conclude this work by demonstrating that the formulas derived here not only predict abundance spectra but that they can actually be applied to solve the inversion problem. Using the simulations that have already illustrated the validity of the partial solutions, we have inverted the abundance spectra to yield the relative separation energies. The results are shown in Fig. 6.

The results presented in this work show that evaporative spectra can be used to extract valuable *quantitative* information about the energetics of clusters. The theory is universal in the sense that if the relatively mild conditions imposed during the derivation are fulfilled, it will be valid irrespective of the choice of cluster material and the underlying physical reason for the variations in binding energy. If the dissociation energies extracted from experimental spectra, i.e., the thermal activation energies, are identical to the adiabatic differences in free energies of the mother and daughter clusters, the dissociation energies can be integrated to give the shell energies.

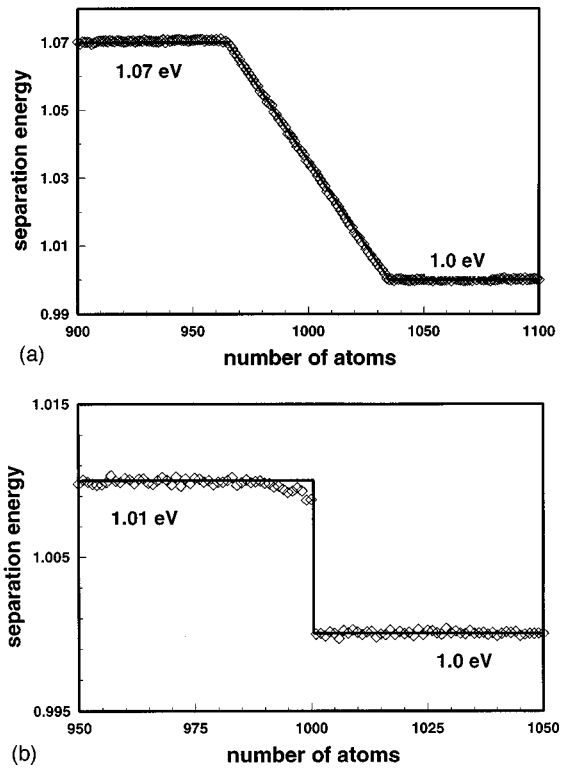

FIG. 6. The separation energies (in eV) as calculated from Eq. (63) in the text. The line is the input curve for the MC simulations also shown in Figs. 3 and 4. The outputs of the simulations were inverted to find the separation energies (diamonds). No fitting parameters were used to find the inverted curve. The overall scale, however, was fixed arbitrarily.

The theory presented here is applicable only if the clusters have certain properties: Decay should be restricted to evaporation of a single type of fragment with no competing decay channels present (thermionic emission, radiative cooling). The dissociation energy should be constant, excluding, e.g., the case of evaporatively freezing clusters. These conditions can be checked by a variety of measurements of ensemble evaporation rates and abundance spectra vs time and the amount and the method of excitation of the clusters.

ACKNOWLEDGMENTS

This work was supported by the Danish National Research Foundation through the research center ACAP. Discussions with T. Dǿssing are gratefully acknowledged.

[1] W. D. Knight, K. Clemenger, W. A. de Heer, W. A. Saunders, M. Y. Chou, and M. L. Cohen, Phys. Rev. Lett. **52**, 2141 (1984).

[2] H. Nishioka, Klavs Hansen, and B. R. Mottelson, Phys. Rev. B **42**, 9377 (1990).

[3] J. Pedersen, S. Bjørnholm, J. Borggreen, K. Hansen, T. P. Martin, and H. D. Rasmussen, Nature (London) **353**, 733 (1991).

[4] T. P. Martin, S. Bjørnholm, J. Borggreen, C. Bréchignac, Ph. Cahuzac, K. Hansen, and J. Pedersen, Chem. Phys. Lett. **186**, 53 (1991).

[5] O. Echt, K. Sattler, and E. Recknagel, Phys. Rev. Lett. **47**, 1121 (1981).

[6] W. Miehle, O. Kandler, T. Leisner, and O. Echt, J. Chem. Phys. **91**, 5940 (1989).

[7] T. P. Martin, T. Bergmann, H. Göhlich, and T. Lange, Chem. Phys. Lett. **172**, 209 (1990).

[8] By the expression ''trivial transition state'' we mean that the molecule/atom interacts with the cluster through a purely attractive potential.

[9] T. P. Martin, Surf. Rev. Lett. **3**, 281 (1996).
[10] F. Chandezon, C. Guet, B. A. Huber, D. Jalabert, M. Maurel, E. Monnand, C. Ristori, and J. C. Rocco, Nucl. Instrum. Methods Phys. Res. B **98**, 482 (1995).
[11] C. Brechignac, P. Cahuzac, F. Carlier, M. De Frutos, and J. P. Roux, Phys. Rev. B **47**, 2271 (1993).
[12] D. M. Brink and S. Stringari, Z. Phys. D **15**, 257 (1990).
[13] R. Casero and J. M. Soler, J. Chem. Phys. **95**, 2927 (1991).
[14] P. Fröbrich, Z. Phys. D **40**, 198 (1997).
[15] K. Hansen, Surf. Rev. Lett. **3**, 597 (1996).
[16] C. E. Klots, Z. Phys. D **21**, 335 (1991). The binding energy-abundance relation is not given explicitly; rather the unimolecular decay probability is calculated.
[17] U. Näher and K. Hansen, J. Chem. Phys. **101**, 5367 (1994).
[18] A. N. Nesmeyanov, *Vapor Pressure of the Chemical Elements* (Elsevier, Amsterdam, 1963).
[19] B. Ernstberger, H. Krause, and H. J. Neusser, Ber. Bunsenges. Phys. Chem. **97**, 884 (1993).
[20] K. Hansen and E. E. B. Campbell, J. Chem. Phys. **104**, 5012 (1996).
[21] B. Weber and R. Scholl, J. Appl. Phys. **74**, 607 (1993).
[22] R. Mitzner and E. E. B. Campbell, J. Chem. Phys. **103**, 2445 (1995).
[23] U. Frenzel, A. Roggenkamp, and D. Kreisle, Chem. Phys. Lett. **240**, 109 (1995).
[24] U. Frenzel, U. Hammer, H. Westje, and D. Kreisle, Z. Phys. D **40**, 108 (1997).
[25] J. Gspann, in *Physics of Electronic and Atomic Collisions*, edited by S. Datz (North-Holland, Amsterdam, 1982), pp. 79–96; J. Gspann, *Metal Clusters*, edited by F. Träger and G. zu Putlitz (Springer, Berlin, 1986), pp. 43–45.
[26] C. E. Klots, Nature (London) **327**, 222 (1987).
[27] P. A. Hervieux and D. H. E. Gross, Z. Phys. D **33**, 295 (1995).
[28] P. Fröbrich, Phys. Lett. A **202**, 99 (1995).
[29] S. Frauendorf, Z. Phys. D **35**, 191 (1995).
[30] G. F. Bertsch, N. Oberhofer, and S. Stringari, Z. Phys. D **20**, 123 (1991).
[31] V. Weisskopf, Phys. Rev. **52**, 295 (1937).
[32] K. Hansen and M. Manninen, J. Chem. Phys. **101**, 10 481 (1994).
[33] C. Bréchignac, Ph. Cahuzac, J. Leygnier, and J. Weiner, J. Chem. Phys. **90**, 1492 (1989).
[34] F. Chandezon, P. M. Hansen, C. Ristori, J. Pedersen, J. Westergaard, and S. Bjørnholm, Chem. Phys. Lett. **277**, 450 (1997).
[35] A. Bohr and B. R. Mottelson, *Nuclear Structure II* (Benjamin, New York, 1975).
[36] M. Brack, O. Genzken, and K. Hansen, Z. Phys. D **21**, 65 (1991).
[37] O. Genzken and M. Brack, Phys. Rev. Lett. **67**, 3286 (1991).
[38] Formally this derivation breaks down at temperatures larger than one-third of the separation energy (in the harmonic approximation). We will not deal with such situations.
[39] K. Hansen, H. Hohmann, R. Müller, and E. E. B. Campbell, J. Chem. Phys. **105**, 6088 (1996).
[40] K. Hansen, H. Hohmann, R. Müller, and E. E. B. Campbell, Z. Phys. D **40**, 361 (1997).
[41] S. Bjørnholm, J. Borggreen, O. Echt, K. Hansen, J. Pedersen, and H. D. Rasmussen, Z. Phys. D **19**, 47 (1991).